Neuron 51, 227–238, July 20, 2006 ©2006 Elsevier Inc. DOI 10.1016/j.neuron.2006.06.017

# A Cooperative Switch Determines the Sign of Synaptic Plasticity in Distal Dendrites of Neocortical Pyramidal Neurons

**Per Jesper Sjöström[1,2,*] and Michael Häusser[1,2]**
[1] Wolfson Institute for Biomedical Research
[2] Department of Physiology
University College London
London WC1E 6BT
United Kingdom

## Summary

**Pyramidal neurons in the cerebral cortex span multiple cortical layers. How the excitable properties of pyramidal neuron dendrites allow these neurons to both integrate activity and store associations between different layers is not well understood, but is thought to rely in part on dendritic backpropagation of action potentials. Here we demonstrate that the sign of synaptic plasticity in neocortical pyramidal neurons is regulated by the spread of the backpropagating action potential to the synapse. This creates a progressive gradient between LTP and LTD as the distance of the synaptic contacts from the soma increases. At distal synapses, cooperative synaptic input or dendritic depolarization can switch plasticity between LTD and LTP by boosting backpropagation of action potentials. This activity-dependent switch provides a mechanism for associative learning across different neocortical layers that process distinct types of information.**

## Introduction

Learning and memory, as well as the refinement of cortical maps during development, are thought to be due to changes in the strength of individual synaptic connections between neurons (Katz and Shatz, 1996; Malenka and Nicoll, 1999). Hebb postulated that such synaptic strengthening occurs during persistent simultaneous activity in pre- and postsynaptic neurons (Hebb, 1949). At both hippocampal (Magee and Johnston, 1997) and neocortical (Markram et al., 1997b; Sjöström et al., 2001) synapses, repeated coincidence of EPSPs and postsynaptic action potentials (APs) results in long-term potentiation (LTP), thus satisfying the Hebbian postulate. Backpropagation of the AP into the dendrites appears to be a critical requirement for triggering changes in strength at many synapses (Linden, 1999). This coincidence detection depends at least in part on supralinear $Ca^{2+}$ influx through NMDA receptors (Koester and Sakmann, 1998; Yuste and Denk, 1995) and on nonlinear summation mediated by voltage-gated dendritic channels (Magee and Johnston, 1997; Stuart and Häusser, 2001). However, the backpropagating AP (bAP) is typically strongly attenuated in distal dendrites of pyramidal neurons (Stuart et al., 1997; Stuart and Häusser, 2001). This suggests that bAP-dependent learning rules may be different at proximal and distal synapses (Froemke et al., 2005; Goldberg et al., 2002; Golding et al., 2002; Lisman and Spruston, 2005; Sourdet and Debanne, 1999). Neocortical layer 5 (L5) pyramidal neurons represent an excellent model system for addressing this issue, since these neurons have a large apical dendritic arbor that extends for hundreds of microns across several cortical layers, and since they receive two well-defined inputs, making synapses at different dendritic locations: the vast majority of L5-to-L5 synapses are on the proximal, basal dendritic tree (Markram et al., 1997a), while L2/3-to-L5 synapses are found on the apical as well as the basal dendrites (Thomson and Bannister, 1998). However, the consequences of synaptic location for plasticity exhibited by these two distinct inputs are not known.

Here we have investigated how plasticity rules for L2/3 and L5 inputs to L5 pyramidal neurons depend on the dendritic location of synaptic contacts and their interaction with the local excitable properties of the dendritic tree. We have used a combination of quadruple simultaneous patch-clamp recordings (Sjöström et al., 2001), dendritic patch-clamp recordings (Stuart and Sakmann, 1994), two-photon imaging (Koester and Sakmann, 1998; Yuste and Denk, 1995), and modeling of reconstructed neurons (Markram et al., 1997a; Redman and Walmsley, 1983) in order to test identical plasticity protocols at the two different unitary inputs and relate the outcome to the location of identified synaptic contacts and the dendritic $Ca^{2+}$ signals associated with plasticity induction. We found that, surprisingly, the same AP-EPSP pairing protocol generates LTP at proximal L5-to-L5 connections, but LTD at distal L2/3-to-L5 connections, thus creating a gradient along the apical dendrite for the polarity of plasticity. We demonstrate that this gradient is defined by the efficacy of AP backpropagation to the respective synaptic sites, since dendritic depolarization or cooperative synaptic input can rescue LTP at distal synapses in a manner which is tightly linked to the boosting of AP backpropagation into the distal dendritic tree. We also show that these electrical interactions are reflected in terms of dendritic $Ca^{2+}$ signals. Our findings provide a dendritic mechanism by which inputs in deeper cortical layers can regulate plasticity at inputs in more superficial layers.

## Results

We compared plasticity of synaptic inputs mediated by two distinct input pathways in L5 pyramidal neurons by making simultaneous recordings from L5 neurons and presynaptic L5 and L2/3 pyramidal neurons. We used the same plasticity protocol at both synaptic connections, consisting of pairing five EPSPs and APs at 50 Hz. This frequency is below the critical frequency for evoking $Ca^{2+}$ spikes in pyramidal cell dendrites (Larkum et al., 1999a). Pairing EPSPs and APs at L5-to-L5 connections produced robust LTP (Figure 1A; after/before 140% ± 6%, n = 34; Markram et al., 1997b; Sjöström et al., 2001). In contrast, when the identical pairing protocol was applied at unitary L2/3-to-L5 connections, this

*Correspondence: j.sjostrom@ucl.ac.uk

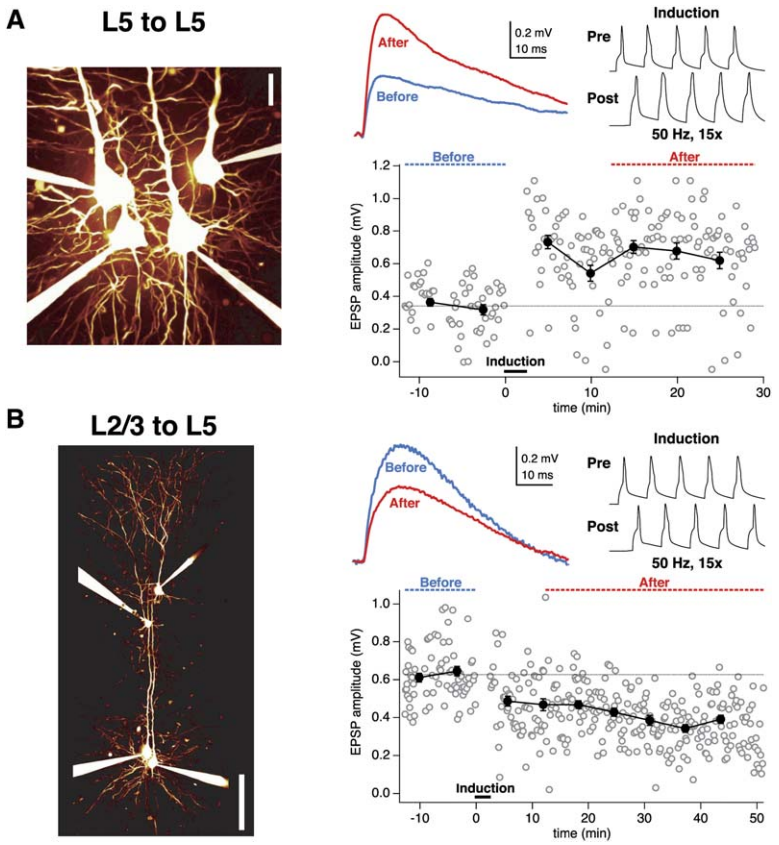


Figure 1. AP-EPSP Pairing Evokes LTP at an L5-to-L5 Connection, but LTD at an L2/3-to-L5 Connection

(A) AP-EPSP pairing at a unitary L5-to-L5 connection resulted in LTP. After the baseline period (blue dotted line and blue trace, top middle inset), pre- and postsynaptic 50 Hz AP trains were paired (pre leading before post by 10 ms; top right inset). The post-pairing responses (red dotted line and red trace, top middle inset) were significantly potentiated (after/before = 195%, $p < 0.001$; EPSP rise time = 1.9 ms), in agreement with prior studies (Markram et al., 1997b; Sjöström et al., 2001). (Left) Illustration of recording configuration for L5-to-L5 pairs.

(B) The same conditions and induction protocol as in (A) in this L2/3-to-L5 paired recording, however, resulted in significant LTD (after/before = 63%, $p < 0.001$; EPSP rise time 3.5 ms). (Left) Recording configuration.

did not produce LTP (106% ± 9%, n = 19; $p < 0.001$ compared to L5-to-L5 connections). Indeed, for many L2/3-to-L5 pairs this induction protocol resulted in LTD (Figure 1B).

### Identifying the Dendritic Location of Synapses

Synaptic contacts of L5-to-L5 and L2/3-to-L5 connections tend to be made at different locations in the dendritic tree of L5 pyramidal neurons (Markram et al., 1997a; Thomson and Bannister, 1998). We used a combination of computer modeling and direct visualization of contacts to identify the location of synaptic contacts in our connected pairs. Cable theory predicts that EPSP rise time should be correlated with dendritic location of the active synaptic contacts (Rall, 1967). We made detailed compartmental models based on three-dimensional reconstructions of biocytin-filled L5 pyramidal neurons from our paired recordings (Figure 2A; see the Experimental Procedures). Results from simulations using such a model are shown in Figures 2B and 2C, which allow us to quantitatively predict the relationship between synaptic location and somatic EPSP rise time under the conditions of our experiments for the entire range of possible synaptic locations.

We validated this approach experimentally by directly identifying putative synaptic contacts during some recordings by imaging contacts made by the presynaptic axon with the postsynaptic target using two-photon laser-scanning microscopy (2PLSM) of neurons filled with fluorescent dye (see Figure S1 in the Supplemental Data). Alternatively, we filled neurons with biocytin and identified putative synaptic contacts using bright-field microscopy of fixed and histologically processed neurons (Figure 2A). Across the population, the distance from the soma of visually identified putative synapses was tightly correlated with somatic EPSP rise time (Figure 2E). This provides a model-independent index relating somatic EPSP rise time and synaptic location, which closely agrees with the prediction of our simulations (Figure 2C). Finally, we used this index to verify that—as predicted on the basis of anatomy (Markram et al., 1997a; Thomson and Bannister, 1998)—the location of functional L2/3-to-L5 synapses (rise time 3.0 ± 0.4 ms; n = 19) was on average significantly farther from the soma than that of L5-to-L5 synapses (2.2 ± 0.2 ms, n = 34, $p < 0.05$).

### The Sign of Plasticity Depends on Synaptic Location

Next, we used EPSP rise time as an index of synaptic location to determine if location is correlated with the outcome of the plasticity protocol. Across all unitary L5-to-L5 and L2/3-to-L5 connections, we found a clear relationship between the sign of plasticity and the synaptic location (estimated by EPSP rise time). Thus, proximal inputs with fast-rising EPSPs exhibited classical Hebbian LTP, whereas distal inputs with slow-rising EPSPs underwent LTD (Figure 3). In a subset of experiments, where we also identified putative synaptic contacts (Figure S1), we could demonstrate directly that the sign of plasticity depended on the distance of synaptic contacts from the soma (inset, Figure 3). We confirmed and extended these results by activating inputs at a range of distances from the soma using extracellular

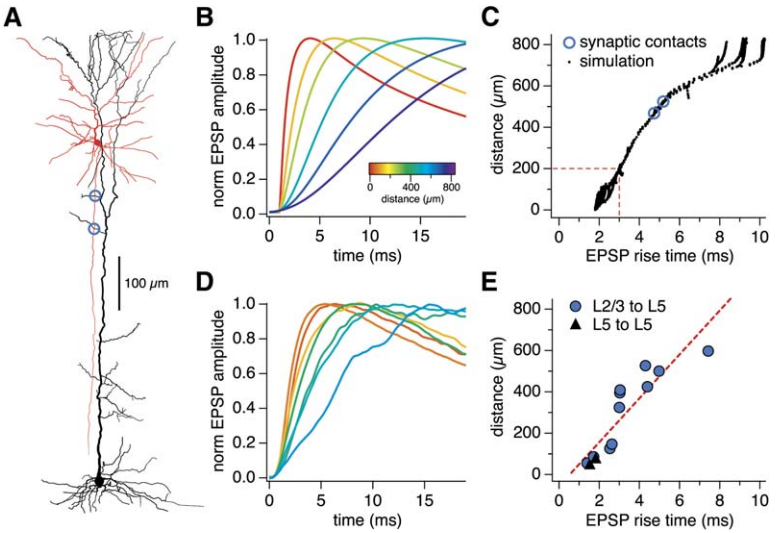


Figure 2. Identifying Synaptic Locations from EPSP Rise Time and Morphology

(A) Reconstruction of an L2/3-to-L5 connected pair (blue circles, putative synaptic contacts).

(B) Using a computer model of the reconstructed L5 neuron in (A), calibrated to the actual EPSP rise time (5.0 ms) of this paired recording by assuming equal contribution of the two putative synaptic contacts, we simulated the activation of synapses in different locations of the dendritic tree. This gave rise to EPSPs with different rise times (color-coded according to synapse location).

(C) Based on this simulation, we predicted the relationship between distance and somatic EPSP rise time for many synaptic locations. Dashed line: 3 ms cut-off that defines proximal versus distal inputs (see text).

(D) In several paired recordings, putative synaptic contacts were identified (cf. Figure S1), which enabled the verification of the simulation (cf. [B]).

(E) The mean location of putative synaptic contacts correlated well (r = 0.89) with the somatic EPSP rise time in L5-to-L5 (black triangles) and L2/3-to-L5 (closed blue circles) paired recordings (n = 13), thus corroborating the model prediction (cf. [C]).

stimulation (Figure 3). While overall the degree of plasticity was statistically different between L2/3-to-L5 and L5-to-L5 pathways, the overlap in the distribution of synaptic locations and the strong correlation with rise time (Figure 3) indicate that synaptic location in the dendritic tree, rather than input origin per se, is the major determinant of plasticity.

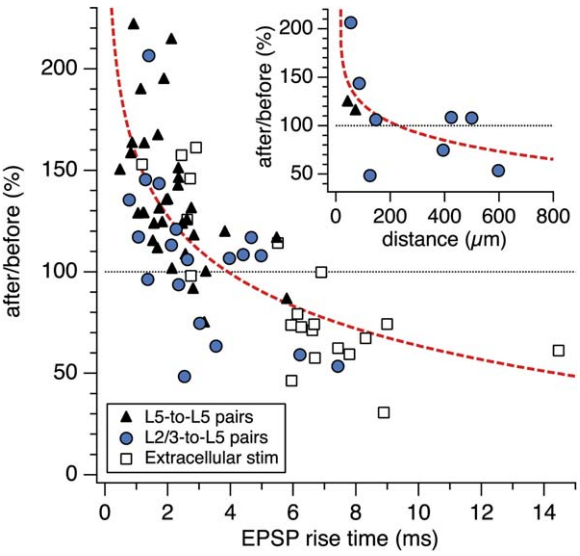


Figure 3. Synaptic Location Determines the Sign of Plasticity

AP-EPSP pairing in L5-to-L5 pairs (closed black triangles, n = 34), L2/3-to-L5 pairs (closed blue circles, n = 19), and extracellular stimulation experiments (open black squares, n = 21) resulted in LTP of proximal inputs (somatic EPSP rise time < 3 ms; 137% ± 4.9%, n = 46), but evoked LTD of distal input (somatic EPSP rise time > 3 ms; 80.2% ± 4.5%, n = 28, p < 0.001). (Inset) In agreement with this, the sign of plasticity was inversely correlated with average distance of putative synaptic contacts (n = 11; also see Figure S1). Dashed red lines are power law fits.

## Converting LTD to LTP at Distal Synapses

To determine if distal inputs, which tend to exhibit LTD, can be converted to exhibit LTP, we selectively activated distal synaptic inputs near the apical tuft of L5 neurons using extracellular stimulation, restricting ourselves to the most distal inputs with a rise time >3 ms (corresponding to >200 μm from the soma, cf. Figure 2C). Since it takes an AP several milliseconds to backpropagate the entire length of the apical dendrite (Stuart and Sakmann, 1994), it is conceivable that this delay might push pre- and postsynaptic spike pairings out of the temporal window for LTP and into that of LTD (Sjöström et al., 2001). To test this hypothesis, we modified our pairing protocol to evoke postsynaptic spikes 5 ms (instead of 10 ms) after extracellular stimulation near the apical tuft. This compensation of the temporal delay did not switch distal LTD to LTP (data not shown; after/before = 89% ± 5%, EPSP rise time 5.2 ± 0.6 ms, amplitude 0.4 ± 0.1 mV, n = 4). This result indicates that the delay due to AP backpropagation does not underlie the location dependence of plasticity shown in Figure 3, consistent with the observation that precise timing of pre- and postsynaptic spikes has relatively little impact on plasticity evoked by correlated 50 Hz firing (Sjöström et al., 2001).

However, for distal inputs, recruiting more inputs by increasing stimulation strength resulted in large EPSPs that potentiated when paired with APs at 50 Hz (Figures 4A and 4C). To directly verify that this cooperativity rule holds for identified unitary distal inputs, we made paired recordings between L2/3 and L5 pyramidal neurons exhibiting distal synaptic connections, which normally do not potentiate when paired at 50 Hz with APs (Figure 3). When such connections were subjected to the conventional pairing protocol in combination with strong extracellular stimulation to boost the unitary EPSP, these connections exhibited LTP (Figures 4B and 4C). Pooling data from all distal inputs (both paired recordings as well

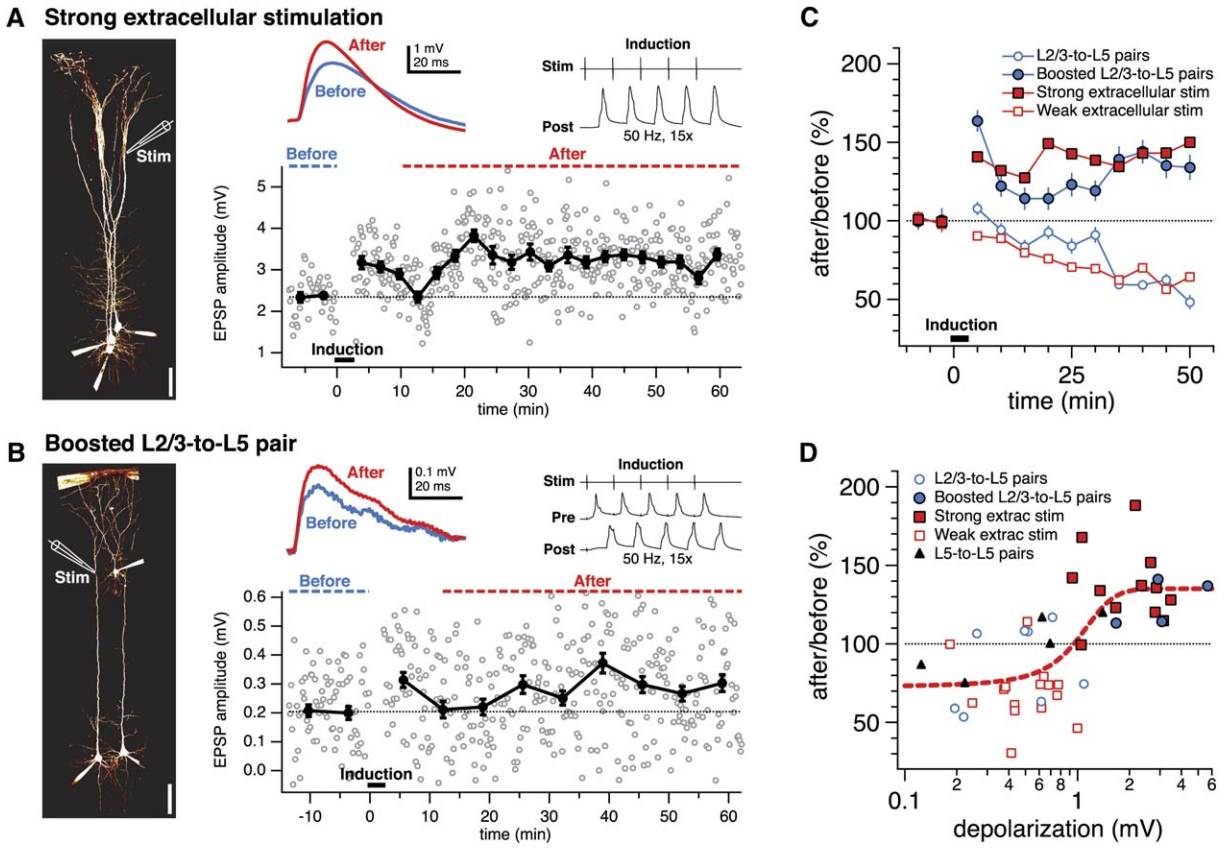


Figure 4. LTP Induction at Distal Synapses Requires Cooperativity among Inputs

(A) Strong extracellular stimulation near the distal dendritic tuft (left) recruited a slow, large EPSP (rise time 5.2 ms) that significantly potentiated when paired with APs at 50 Hz (137%, $p < 0.001$). (Left) Configuration permitted multiple parallel recordings.

(B) A distal L2/3-to-L5 unitary input (rise time 4.2 ms) that was boosted by extracellular stimulation during the induction (compound EPSP 5.7 mV) potentiated significantly after AP-EPSP pairing (137%, $p < 0.001$). (Left) Stimulation electrode placement is illustrated schematically.

(C) Using extracellular stimulation, pairing small distal EPSPs with APs resulted in LTD (closed red squares, 70% ± 5%, n = 15). Recruiting more inputs by increasing extracellular stimulation strength, however, resulted in large EPSPs that potentiated robustly when paired with APs (open red squares, 137% ± 7%, n = 12; $p < 0.001$), demonstrating a cooperativity requirement for distal LTP. Similarly, although distal unitary connections typically depressed (open blue circles, 86% ± 9%, n = 8; cf. Figure 3), boosted distal unitary connections (cf. [B]) significantly potentiated (126% ± 7%, n = 4, $p < 0.05$). (D) For distal inputs, LTD (80% ± 5%, n = 25) was observed below a threshold somatic EPSP amplitude (<1.0 mV). Above this threshold, distal plasticity switched to LTP (126% ± 7%, n = 19; $p < 0.001$). Data is pooled from L5-to-L5 pairs (triangles), L2/3-to-L5 pairs (open blue circles), boosted L2/3-to-L5 pairs (closed blue circles) and extracellular stimulation experiments (open and closed squares). Dashed red line is best fit sigmoid. Only experiments with EPSP rise time > 3 ms (cf. Figure 2) were included in (C) and (D).

as extracellular stimulation), we found that AP-EPSP pairing of distal inputs above a threshold amplitude reliably resulted in LTP (Figure 4D; sigmoid $x_{half}$ = 1.0 mV; sliding t test minimum 1.06 mV; see Experimental Procedures). In other words, the sign of distal plasticity was switched from negative (LTD) to positive (LTP) once a sufficient number of distal inputs cooperated (Figure 4D).

The cooperativity requirement for distal LTP might be due to a need for local dendritic spikes, as was recently found in CA1 pyramidal neurons (Golding et al., 2002), in which case pairing with somatic APs may not be required for LTP of large distal EPSPs. Activating distal EPSPs at 50 Hz in the absence of postsynaptic somatic spiking, however, did not produce LTP, but surprisingly resulted in LTD (Figures 5A and 5B). Postsynaptic 50 Hz spiking in the absence of presynaptic stimulation, on the other hand, did not change synaptic strength (Figure 5B). These results show that, in the absence of postsynaptic spiking, activation of large distal inputs at 50 Hz (but not at 0.1 Hz, our baseline firing rate) results in LTD. We hypothesized that this form of LTD—which apparently depends on pairing presynaptic activity with subthreshold postsynaptic depolarization—was similar to the endocannabinoid-dependent, depolarization-induced LTD previously described at proximal L5-to-L5 synapses (Sjöström et al., 2004). In keeping with this view, the endocannabinoid CB1 receptor blocker AM251 abolished this form of distal LTD (Figure 5B) (Sjöström et al., 2004). Taken together, these results show that in L5 neurons, distally evoked EPSPs undergo LTP when a dual requirement for coincidence with APs and cooperativity among inputs is satisfied. For inputs that are activated at 50 Hz, failure to satisfy either requirement results in LTD.

### Boosting of bAPs Underlies the Switch between Distal LTD and LTP

Can the cooperativity requirement for distal LTP be explained by the boosting of failing bAPs? Backpropagating APs may not be sufficient to unblock NMDA

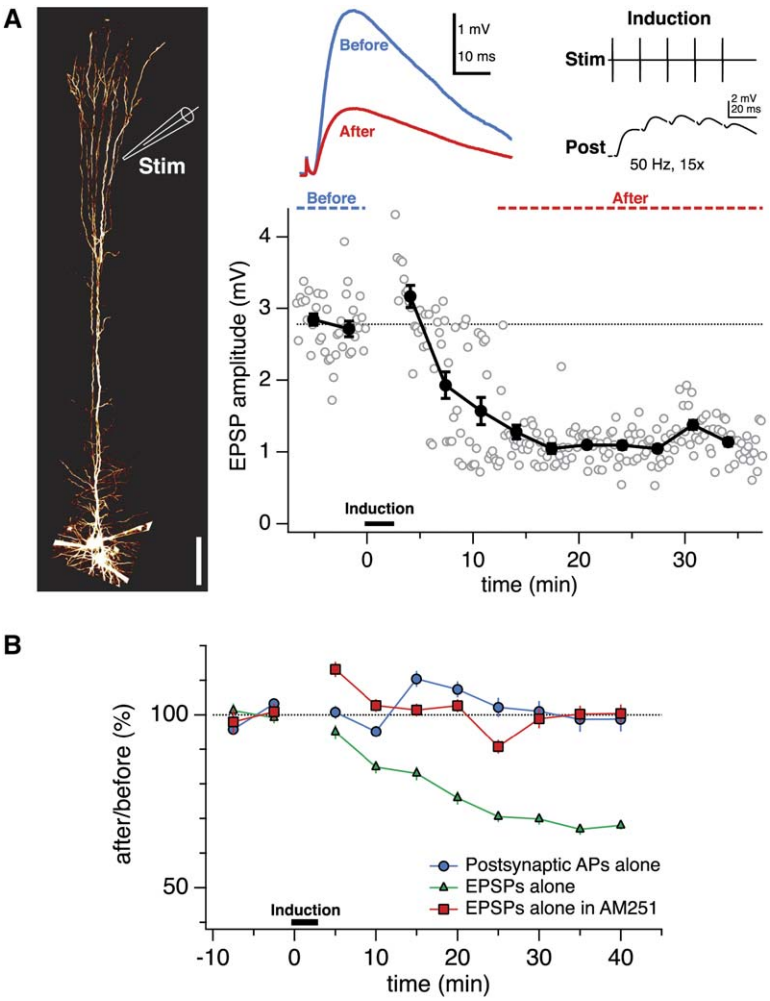


Figure 5. Distal LTD is Endocannabinoid-Dependent

(A) Extracellular 50 Hz stimulation of distal inputs (rise time 3.7 ms) in the absence of somatic spiking resulted in depression (41%, $p < 0.001$). (Left) Recording configuration.

(B) Unpaired distal EPSPs evoked LTD (green triangles, 71% ± 6%, n = 10; cf. Golding et al., 2002) that was abolished by the endocannabinoid CB1 receptor blocker AM251 (Gatley et al., 1996) (red squares, 99% ± 3%, n = 6, $p < 0.01$). Unpaired spike trains (blue circles, 102% ± 6%, n = 10) did not evoke plasticity.

receptors and induce LTP for small distal inputs (Sjöström and Nelson, 2002), since APs backpropagate decrementally (Larkum et al., 1999a, 2001; Stuart et al., 1997; Stuart and Häusser, 2001; Williams and Stuart, 2000), but bAPs may still depolarize the distal dendrites sufficiently to help evoke LTD (Artola et al., 1990; Sjöström et al., 2004). Sufficiently large distal EPSPs, on the other hand, may potentiate because they provide enough dendritic depolarization to boost failing bAPs (Larkum et al., 2001; Stuart and Häusser, 2001; Williams and Stuart, 2000). If so, then small distal EPSPs should potentiate if the bAP is boosted by direct dendritic depolarization (Larkum et al., 2001; Stuart and Häusser, 2001; Williams and Stuart, 2000). In agreement with this, we found that brief subthreshold dendritic current injection in conjunction with the pairing of APs and small distal EPSPs produced LTP (Figure 6). Somatic subthreshold depolarization of the same amplitude and duration, however, did not evoke LTP of small distal EPSPs (Figure 6B), showing that dendritic, but not somatic, depolarization determines the sign of distal plasticity.

To determine whether the efficacy of AP backpropagation is linked to distal LTP induction, we examined how LTP-promoting conditions influenced AP backpropagation. Dendritic depolarization boosted the amplitude and increased the half-width of dendritic bAPs (Figure 7A) in a manner that increased with distance from the soma (Figure 7B), consistent with previous findings (Larkum et al., 2001; Stuart and Häusser, 2001; Williams and Stuart, 2000). To examine bAP boosting in multiple locations on the same neuron and in thin distal dendrites where dendritic recordings are not possible, we used 2PLSM imaging of bAP-induced $Ca^{2+}$ responses (see Experimental Procedures). Supralinear $Ca^{2+}$ signals were generated throughout the distal apical dendritic tree by pairing APs with dendritic depolarizing current injection (supralinearity = 268% ± 68%, n = 19, $p < 0.001$; Figure 7C) or with large EPSPs (100% ± 30%, n = 37, $p < 0.001$; Figure 7B), suggesting that boosting of the otherwise-decaying bAP (Larkum et al., 2001; Stuart and Häusser, 2001; Williams and Stuart, 2000) (see Figure S2) occurs over large parts of the distal dendritic tree. The $Ca^{2+}$ signal, due to large EPSPs in the absence of APs, was minimal (Figure 7D), consistent with the need for somatic APs in LTP induction (Figure 5). As with dendritic recordings (Figure 7B), the boosting of the $Ca^{2+}$ signal was more effective in the distal regions of the dendritic tree (Figure 7E), where bAP failure is most prominent (Larkum et al., 1999a, 2001; Stuart and Häusser, 2001; Williams and Stuart, 2000) (cf. Figure S2). Pairing of unboosted bAPs and small distal

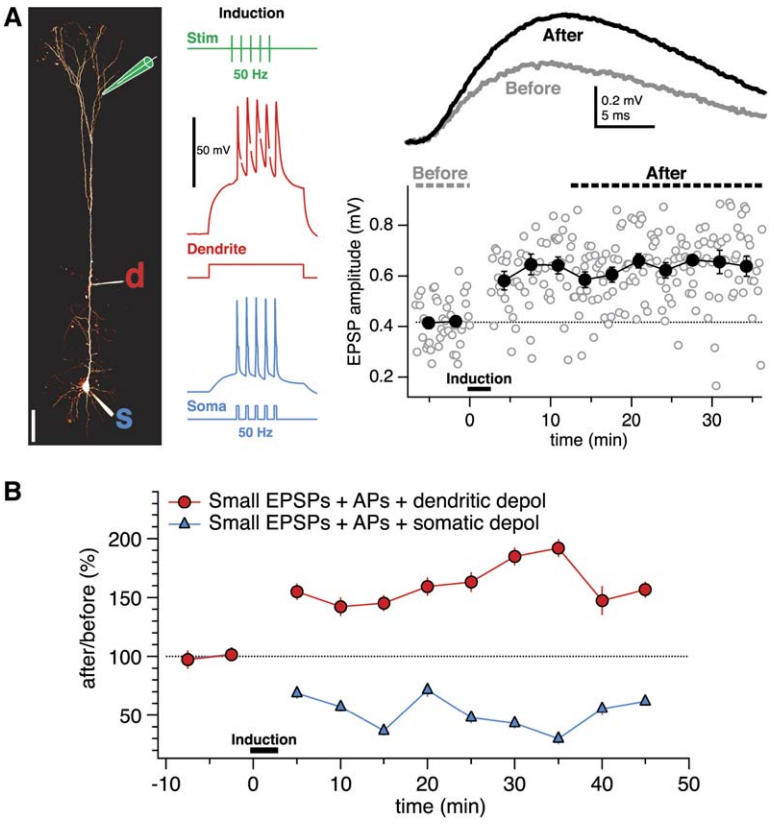


Figure 6. Dendritic Depolarization Switches Distal Plasticity from LTD to LTP

(A) AP-EPSP pairing in conjunction with a brief subthreshold dendritic current injection (0.4 nA, 200 ms, red trace) resulted in LTP of a small, distal input (rise time 4.9 ms). (Left) Recording configuration, also showing sample LTP induction traces (stimulus electrode, green; dendrite, red, "d;" soma, blue, "s").

(B) Pairing of APs and EPSPs in the presence of a brief subthreshold dendritic current injection (247 ± 22 μm from the soma) evoked LTP of small distal inputs (<1 mV; red circles; 163% ± 7%, n = 5). The corresponding amount of subthreshold current injected into the soma, however, resulted in LTD (blue triangles; 88% ± 8%, n = 3). The subthreshold dendritic (0.35 ± 0.03 nA) and somatic (0.31 ± 0.01 nA) current injections were not significantly different ($p = 0.36$). These results demonstrate that dendritic, but not somatic, depolarization switches distal plasticity from LTD to LTP ($p < 0.001$).

EPSPs (<1.01 mV; Figure 4C), however, did not result in supralinear $Ca^{2+}$ influx (−2% ± 8%, n = 9; EPSP amplitude 0.37 ± 0.2 mV; data not shown), consistent with the requirement for sufficiently large EPSPs in bAP boosting and in LTP (Figures 4C and 4D). In five cells, we increased the extracellular stimulation strength stepwise to determine the threshold for AP-EPSP-induced supralinear $Ca^{2+}$ signals. This threshold (sigmoid $x_{half}$ = 1.1 ± 0.32 mV) matched that of LTP induction (see above and Figure 4D). Taken together, these results identify a depolarization threshold for distal LTP (Figures 4C and 4D) that is due to a requirement for boosting of the bAP.

### LTP at Proximal Synapses also Requires Reliable AP Backpropagation

If the cooperativity requirement of distal LTP results from the need to boost failing bAPs, then weakening AP propagation into basal dendrites should in turn affect plasticity of proximal inputs in a converse manner. We therefore examined the effect of delivering strong, brief postsynaptic hyperpolarization on plasticity at proximal connections during our 50 Hz pairing protocol. First, we investigated whether this manipulation indeed impairs backpropagation into basal dendrites during the pairing protocol, using dendritic $Ca^{2+}$ signals as an index of backpropagation. Strong, brief hyperpolarization caused a reduction in the dendritic $Ca^{2+}$ signal associated with backpropagating APs, and this reduction increased progressively along both the basal and apical dendrites with distance from the soma, while leaving the axonal signal unaffected (Figures 8A and 8B). These results are thus consistent with impaired dendritic backpropagation due to somatic hyperpolarization. Next, we showed that AP-EPSP pairing during the hyperpolarization abolished LTP at proximal connections (Figures 8C and 8D; cf. Markram et al., 1997b; Sjöström et al., 2001). This result is in keeping with the view that reliability of AP backpropagation determines plasticity in L5 neurons, regardless of synapse location.

While somatic hyperpolarization abolishes LTP due to AP-EPSP pairing at proximal synapses (Figures 8A, 8C, and 8D) (Sjöström et al., 2001), it does not switch plasticity from LTP to LTD. This is perhaps because even failing bAPs still provide sufficient depolarization at proximal synapses to produce a balance between LTP and LTD, which results in no net plasticity. If so, then unpaired proximal inputs should show LTD, just like distal inputs (Figure 5). Consistent with this view, strong 50 Hz extracellular stimulation of proximal inputs resulted in LTD (Figure S3). This LTD required strong stimulation, as it is not observed with unitary connections (Markram et al., 1997b; Sjöström et al., 2003). The dual need for presynaptic high-frequency activity and strong postsynaptic depolarization to evoke LTD at proximal synapses (Figure S3) is similar to the distal LTD observed in the absence of bAPs (Figure 5), and it is also in keeping with prior results showing that LTD requires presynaptic activity paired with sufficiently strong postsynaptic depolarization (Sjöström et al., 2003, 2004). Taken together, these results confirm the key importance of backpropagation in regulating synaptic plasticity, and they suggest that failing or absent bAPs affect plasticity of proximal and distal synapses in a similar manner.

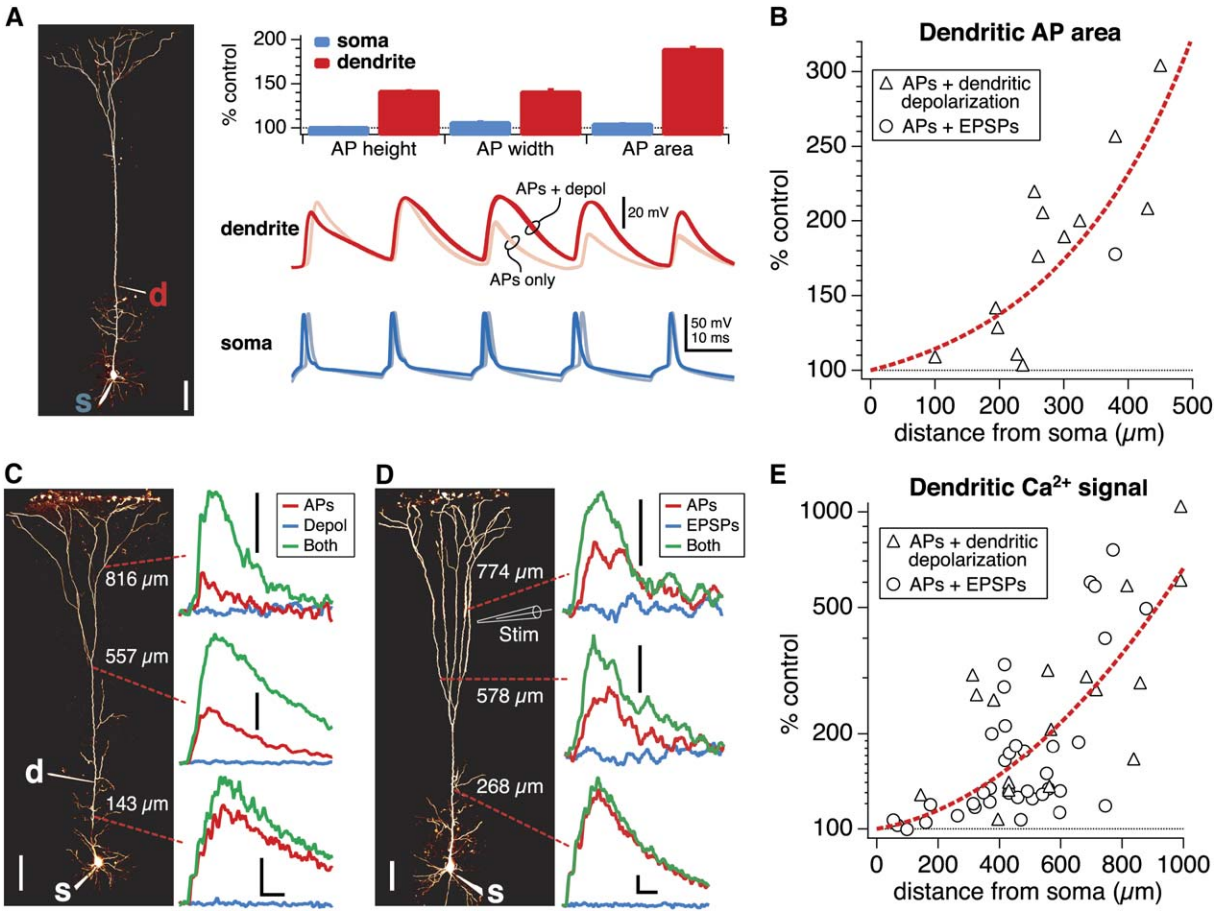


Figure 7. Conditions that Evoke Distal LTP also Boost bAPs

(A) Amplitude, width, and area of bAPs were increased by a 0.4 nA subthreshold dendritic current injection (red bars, top, and red traces in middle). At the soma, the effect on the AP was moderate (blue bars, top, and blue traces at bottom). Traces with 0.4 nA subthreshold current injection are represented with darker colors than control traces (middle, "APs + depol," and bottom). (Left) Dendritic recording ("d") 301 μm from the soma ("s").

(B) The amount of depolarization-induced bAP boosting increased with dendritic recording distance from the soma (Larkum et al., 1999a, 2001; Stuart and Häusser, 2001). The boosting occurred irrespective of the source of the depolarization (dendritic current injection, triangles; synaptic activation, circles; n = 13 cells total).

(C) (Left) L5 pyramidal cell filled with Fluo-5F and Alexa Fluor 594. (Right) Line scans at three dendritic locations reveal supralinear $Ca^{2+}$ signals (green) when pairing APs with a subthreshold 200 ms long dendritic current injection (0.4 nA, 260 μm from soma, "d") in distal dendrites, compared to the arithmetic sum of the APs (red) and the depolarization alone (blue). Note that boosting is widespread in distal dendrites. In this cell, the simultaneous dendritic recording measured a bAP area boosting of 175% ± 0.4%; compare (B). Scale bars, 100 μm, 20% dG/R, 50 ms.

(D) APs paired with distal large EPSPs also resulted in supralinear $Ca^{2+}$ signals (green) in distal dendrites, as compared with APs (red) and EPSPs (blue). As with plasticity experiments (Figure 4), EPSPs (3.9 mV; rise time 3.2 ms) were evoked by relatively strong extracellular stimulation near the dendritic tuft (stimulation electrode position 740 μm). Note that boosting is not limited to locations close to the stimulation electrode. Scale bars, 2% dG/R, and see (C).

(E) The $Ca^{2+}$ signal boosting due to pairing of APs with depolarization (triangles; 18 positions, four cells) or with large EPSPs (circles; 37 positions, ten cells) increased with distance from the soma, indicating that sufficient dendritic depolarization boosts bAPs throughout the distal apical dendritic tree (Larkum et al., 1999a, 2001; Stuart and Häusser, 2001).

## Discussion

Our results reveal two principles for the organization of synaptic plasticity rules in neocortical L5 pyramidal neurons. First, there is a graded change in the sign and magnitude of plasticity with distance from the soma: whereas high-frequency correlated firing evokes Hebbian LTP at proximal synapses, it surprisingly results in LTD of unitary distal inputs. Second, a voltage-dependent dendritic switch governs plasticity at distal synapses, such that dendritic depolarization switches between LTD and LTP given identical patterns of pre- and postsynaptic activity. These principles are both governed by the amplitude of the backpropagating AP at the sites of the active synapses. Our study thus provides some of the most direct evidence to date that the efficacy of AP backpropagation determines the magnitude and sign of synaptic plasticity in dendrites. The resulting model of plasticity in L5 pyramidal neurons is summarized in schematic form in Figure 9.

### Inverted Sign of Plasticity at Distal Synapses

We show that the same standard AP-EPSP pairing protocol can produce LTP at proximal synapses and LTD at distal synapses. To our knowledge, such an inversion of the sign of plasticity depending on dendritic distance

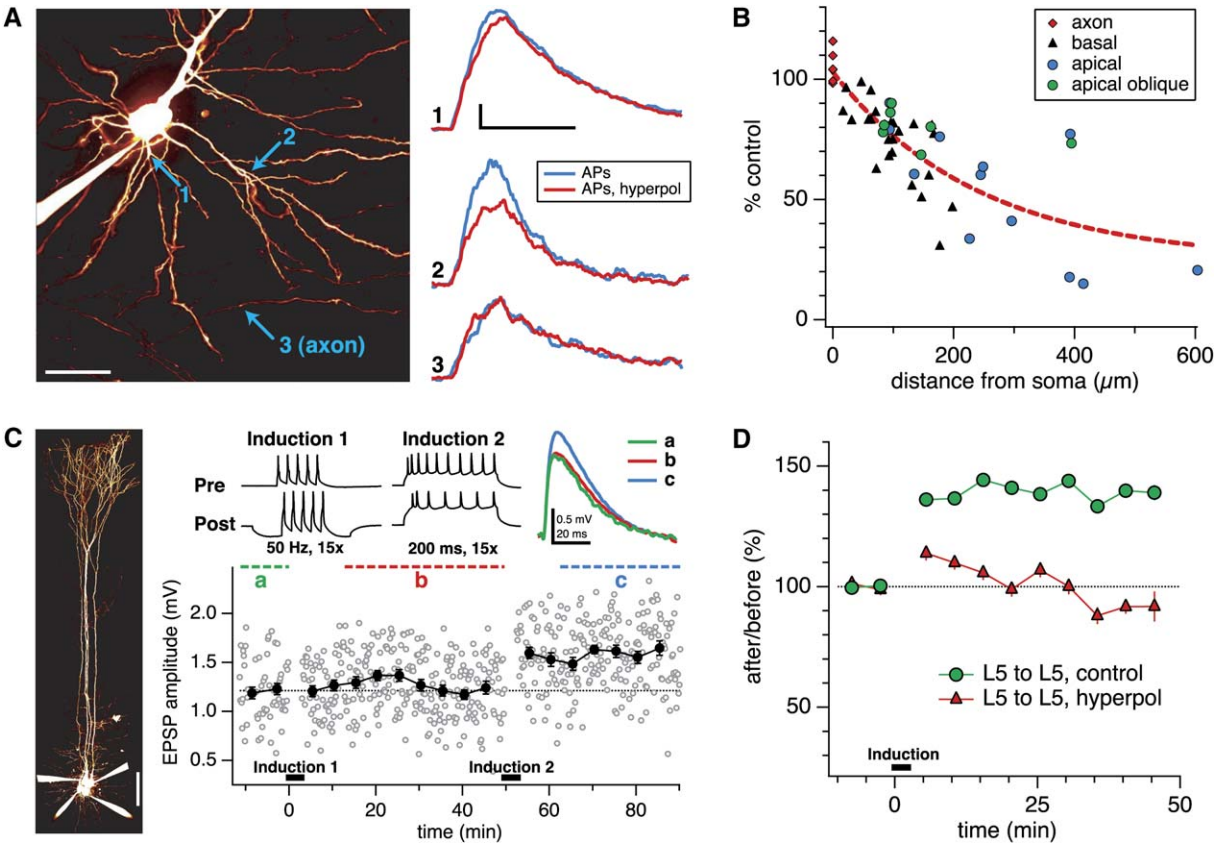


Figure 8. Somatic Hyperpolarization Reduces Basal Dendritic AP-Evoked $Ca^{2+}$ Signals and Abolishes Proximal LTP

(A) (Left) L5 pyramidal cell filled with Fluo-5F and Alexa Fluor 594. (Right) Line scans in basal dendritic locations 1 (21 μm from soma) and 2 (92 μm) reveal reduced $Ca^{2+}$ signals for APs paired with hyperpolarization (red; −0.34 nA, 200 ms, −23 mV max deflection) compared with APs alone (blue). Note the difference in the effect at locations 1 and 2, as well as the absence of an effect in the axon (location 3, 147 μm). Scale bars, 50 μm, 20% dG/R, 200 ms.

(B) AP-evoked $Ca^{2+}$ signals in dendrites, but not in axons, are reduced more by hyperpolarization as the distance from the soma increases. This data is consistent with a hyperpolarization-induced reduction in the reliability of AP propagation into the basal (n = 25) as well as the apical (n = 12) and apical oblique (n = 7) dendritic arbors, but not into the axon (n = 6). Data was collected from five cells. Axonal line scans, indicated at origin for clarity, were acquired 129 ± 14 μm from soma.

(C) In a connected L5-to-L5 pair, strong postsynaptic hyperpolarization during 50 Hz pairing (Induction 1; −0.41 nA, 200 ms) abolished LTP (Sjöström et al., 2001). The same connection subsequently potentiated due to a strong LTP induction protocol (Induction 2; 0.7 nA, 200 ms; 130%, $p < 0.001$), demonstrating that its ability to express LTP was not compromised. Scale bar, 100 μm.

(D) Somatic hyperpolarization blocked LTP in L5-to-L5 pairs (red triangles; n = 6) as compared with controls without hyperpolarization (green circles; n = 34).

has not been demonstrated previously. A recent study in L2/3 pyramidal neurons (Froemke et al., 2005) showed that the temporal window of spike timing-dependent plasticity is different at proximal and distal synapses, leading to different degrees of potentiation or depression, but did not demonstrate a difference in sign of plasticity using the same protocol. Our results indicate that in L5 pyramidal neurons, synaptic location is a critical determinant not simply of the extent, but also of the polarity of plasticity at each given synapse. This finding may help to explain some of the notorious variability in the outcome of plasticity experiments, where synaptic location is normally not rigorously controlled.

### A Dendritic Switch for Regulating Plasticity at Distal Synapses

We demonstrate that distal synapses—which normally undergo LTD when paired with bAPs—undergo LTP in the presence of either cooperative synaptic input or dendritic depolarization. We show that this dendritic switch for plasticity is directly linked to the boosting of bAPs by dendritic depolarization. Magee and Johnston (1997) demonstrated that reliable AP backpropagation is critical for LTP induction in CA1 pyramidal neurons when pairing APs and EPSPs. Several studies have also shown that such AP-EPSP pairing can boost AP backpropagation in a manner that depends on nonlinear recruitment of dendritic voltage-gated $Na^+$ channels (Bernard and Johnston, 2003; Magee and Johnston, 1997; Stuart and Häusser, 2001; Watanabe et al., 2002), but how such boosting is converted into changes in synaptic strength is not well understood, particularly at distal synapses. We show that the same stimuli that boost bAPs also promote the conversion of LTD to LTP at distal synapses, with a close correspondence in the threshold amplitude of EPSPs required to boost backpropagation and trigger the plasticity switch. This finding directly links the mechanism for electrical

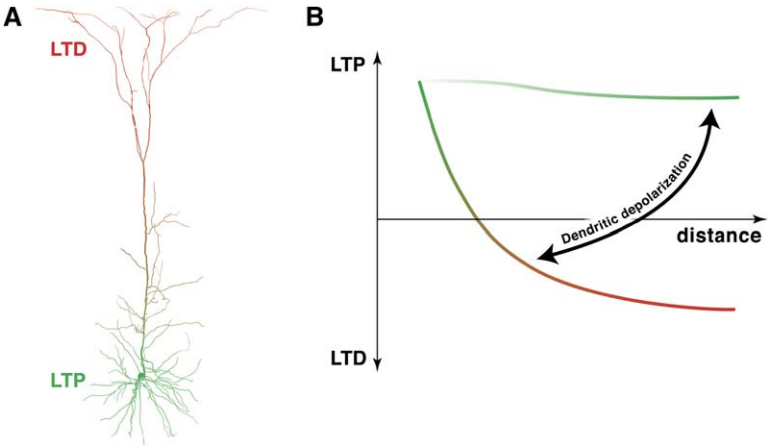


Figure 9. A Dendritic Switch Providing a Learning Rule for Distal Dendritic Long-Term Plasticity

(A) Proximal inputs onto an L5 pyramidal cell are relatively more prone to LTP (green) than distal dendritic inputs, which tend to undergo LTD (red).

(B) Sufficient depolarization of the apical dendrite switches distal plasticity from LTD to LTP. Dendritic depolarization even relatively close to the soma can switch the mode of plasticity at the distal apical dendrite.

coincidence detection in dendrites to synaptic plasticity. We further demonstrate that activation of the plasticity switch is linked to highly supralinear increases in dendritic $Ca^{2+}$, which—given the well-established role of postsynaptic $Ca^{2+}$ elevations in the induction of long-term plasticity (Cummings et al., 1996; Hansel et al., 1997)—may itself influence synaptic plasticity. Our results also provide a mechanism for cooperativity in strengthening distal synaptic inputs, a well-known feature of LTP (Debanne et al., 1996; Hebb, 1949; Levy and Steward, 1979; McNaughton et al., 1978).

Importantly, this plasticity switch is a specifically dendritic feature, since it relies on modulation of AP backpropagation (Hoffman and Johnston, 1999; Stuart et al., 1997). In principle, the mechanisms we describe may operate in any neuron exhibiting decremental AP backpropagation in conjunction with the expression of dendritic voltage-gated $Na^{+}$ channels (Bernard and Johnston, 2003; Stuart and Häusser, 2001). Neurons with different dendritic branching patterns or distributions of dendritic voltage-gated channels, such as hippocampal CA1 (Golding et al., 2002; Magee and Johnston, 1997) or neocortical L2/3 pyramidal neurons (Froemke et al., 2005), may exhibit a different balance and spatial distribution of learning rules. In CA1 pyramidal neurons, for example, somatic APs have little or possibly no impact on LTP of distal inputs, while local dendritic spikes play a prominent role (Golding et al., 2002). In L5 pyramidal neurons, however, somatically evoked bAPs play a critical role in the induction of LTP (Figure 5), and reliability of AP backpropagation determines the sign of plasticity of distal inputs (Figures 6 and 7). This difference may be related in part to the much higher density of A-type potassium channels in distal CA1 dendrites (Hoffman et al., 1997) as compared with L5 dendrites (Bekkers, 2000; Korngreen and Sakmann, 2000).

In the intact brain, where background synaptic activity is more prominent (Destexhe et al., 2003), the transition point between LTP and LTD along the apical dendrite may be tuned by the balance between excitation and inhibition and by their relative distribution along the dendrite. The additional shunt expected from background activity should influence the electrotonic structure of the dendritic tree as well as AP backpropagation (Destexhe et al., 2003) and thus may also affect the activity threshold for the transition between LTP and LTD. Nevertheless, boosting of AP backpropagation by synaptic input has recently been demonstrated in apical dendrites of L2/3 neocortical pyramidal neurons in vivo (Waters and Helmchen, 2004). This suggests that both the efficacy of backpropagation and the level of synaptic input in vivo are within the range that allows effective gating of the cooperative switch, and therefore that this mechanism can be used to regulate the sign of distal dendritic plasticity in vivo.

### Functional Implications

Plasticity is notoriously sensitive to the details of the experimental protocol. We have studied the effect of one particular pairing protocol on synaptic efficacy in young animals. Using other induction frequencies or animal ages may lead to other outcomes; for example, different dendritic mechanisms may be engaged. With these provisos, our results have several important implications for the regulation of plasticity and the distribution of synaptic weights in the dendritic tree. Recent theoretical work has suggested that inverse plasticity rules may help equalize synaptic efficacy across the dendritic tree (Goldberg et al., 2002; Rumsey and Abbott, 2004). However, the propensity for proximal LTP and distal LTD that we have found (Figure 9) may instead lead to a distribution of strong proximal and weak distal inputs. In agreement with this, such a distribution of synaptic efficacies was recently described in L5 neurons (Williams and Stuart, 2002). These relatively weak distal inputs thus must act in tight synchrony to trigger somatic AP output, potentially aided by the generation of dendritic spikes (Golding and Spruston, 1998; Larkum et al., 1999b; Schiller et al., 1997; Williams and Stuart, 2002, 2003).

Functionally, the predisposition of distal synapses for LTD may help ensure the requirement for tight coincident activation of distal inputs in evoking somatic spike output by keeping distal inputs small relative to the threshold for spike generation (Schiller et al., 1997; Williams and Stuart, 2002). In addition, the existence of distal LTD even in the presence of somatic spiking can weaken unreliable and poorly correlated distal inputs by penalizing those distal connections that intermittently fail to satisfy the cooperativity criterion for LTP (discussed below). Even quite strong somatic hyperpolarization cannot promote a similar form of LTD at proximal synapses (Figure 8), highlighting the

location-specific differences in plasticity between proximal and distal inputs.

Cooperative LTP, on the other hand, may reward inputs that act in synchrony and can thus promote associative learning (Hebb, 1949; Levy and Steward, 1979; McNaughton et al., 1978). Since we have shown that distal LTP can be gated by relatively proximal depolarization, our results demonstrate a mechanism for associative learning not just within but also across neocortical layers. This possibility is intriguing since input functionality varies with location in L5 neurons: proximal inputs are mostly of local origin (Markram et al., 1997a; Thomson and Bannister, 1998), whereas L1 inputs onto the apical tuft provide feedback from higher cortical regions (Coogan and Burkhalter, 1990) and thus carry distinct information compared to local inputs. In principle, proximal L2/3-to-L5 connections could therefore gate LTP and "instruct" learning at more distal L1-to-L5 inputs. The state-dependent switch between LTD and LTP at distal synapses may thus both regulate synaptic efficacy as a function of network activity and provide a means for associating and storing information carried by synchronous activity in different cortical layers.

## Experimental Procedures

### Slice Preparation and Electrophysiology

Neocortical brain slices were prepared according to standard techniques (Sjöström et al., 2001). All procedures conformed to the UK Animals (Scientific Procedures) Act 1986. Two- to three-week-old rats were anesthetized with isoflurane and decapitated, and the brain was rapidly removed into ice-cold artificial cerebrospinal fluid (ACSF), containing the following in mM: NaCl, 125; KCl, 2.5; $MgCl_2$, 1; $NaH_2PO4$, 1.25; $CaCl_2$, 2; $NaHCO_3$, 26; Dextrose, 25; osmolality 315–320 mOsm, bubbled with 95% $O_2$/5% $CO_2$. Acute sagittal slices (300 μm) were obtained with a DTK-1000 Microslicer (Dosaka, Japan) or a VT1000S microtome (Leica Microsystems, Germany) and were moved to 37°C ACSF for 10 min, after which they were allowed to cool to room temperature. All experiments were carried out at 32°C–35°C. Patch pipettes for somatic (5–8 MΩ) and dendritic (15–25 MΩ) whole-cell recordings were pulled on a DMZ Universal Puller (Zeitz, München, Germany) or a PC-10 puller (Narishige, Japan) and filled with (in mM) KCl, 20; K-Gluconate, 100; K-HEPES, 10; MgATP, 4; NaGTP, 0.3; Na-Phosphocreatine, 10; and 0.1% w/v Biocytin, adjusted with KOH to pH 7.2–7.4, and with sucrose to 290–295 mOsm. For 2PLSM imaging (see below), 10–25 μM Alexa Fluor 594 and/or 180 μM Fluo-5F pentapotassium salt (Invitrogen, Carlsbad, CA) were added to the internal solution. No plasticity experiments were performed in the presence of Fluo-5F, to avoid possible $Ca^{2+}$ buffering effects on the induction of plasticity; nor was Fluo-5F ever loaded presynaptically.

Extracellular stimulation electrodes (tip diameters of 2–10 μm) were filled with ACSF and were typically placed in L1 or L2/3 (except for in Figure S3 and a small number of data points in Figure 3, in which case electrode placement was in L5) under direct visual control, approximately 5–50 μm from the apical dendrites of recorded L5 cells. Stimulation electrode position and stimulation strength were adjusted until responses were of the desired amplitude and rise time. In the same manner, polysynaptic responses (of variable latency and/or with multiple peaks) and inhibitory contamination (hyperpolarizing responses and/or dramatic facilitation) were selected against. Collection of baseline responses was only begun once satisfactory responses were obtained (typically 2–10 min). Inhibition was never blocked, to avoid possible effects of tonic GABA blockade on dendritic excitability. In some experiments (Figure 5B), the endocannabinoid CB1 receptor blocker AM251 (Gatley et al., 1996) (Tocris Cookson, UK) was added to the ACSF at 0.9 μM (Sjöström et al., 2003, 2004) to block CB1 receptors.

Whole-cell recordings were obtained using identical BVC-700A amplifiers (Dagan Corporation, Minneapolis, MN) controlled by custom electrophysiology software (Sjöström et al., 2001) running on Igor Pro (WaveMetrics Inc., Lake Oswego, OR). Sweeps were filtered at 10 kHz and acquired using MIO-16E boards (National Instruments, Austin, TX) or ITC-18 boards (InstruTECH, Port Washington, NY) on Macintosh (Apple Computer, Cupertino, CA) or Dell (Dell Computers, Round Rock, TX) computers. Series resistance and capacitance were compensated for dendritic recordings ($R_{series}$ < 50 MΩ).

Pyramidal L2/3 and thick-tufted L5 neurons were identified at 600x magnification (Olympus BX51WI, Olympus, Melville, NY) using infrared Dodt contrast optics (Luigs and Neumann, Ratingen, Germany). We searched for unitary connections using quadruple whole-cell recordings to increase the yield (Figures 1A and 1B), as cortical L2/3-to-L5 and L5-to-L5 connectivity is low (10%–15%) (Song et al., 2005; Thomson and Bannister, 1998). The L2/3-to-L5 connectivity depended steeply on the distance between the L2/3 soma and the L5 apical dendrite (data not shown; see also Thomson and Bannister, 1998), so recorded L2/3 neurons were typically within 50 μm of the nearest L5 apical dendrite. The identity of the neurons was typically verified by morphology, either during the experiment by 2PLSM imaging of Alexa Fluor 594 fluorescence (see below), or after the experiments by biocytin histochemistry (Vectastain ABC Elite kit, Vector Labs, Burlingame, CA). Dendritic recordings were made from L5 neurons at distances up to 450 μm from the soma using standard techniques (Stuart and Häusser, 2001).

### Induction of Long-Term Plasticity

After obtaining giga-ohm seals on four neurons, we established the whole-cell configuration in quick succession to prevent unequal LTP dialysis. Connectivity was assessed by averaging 10–40 traces. APs were evoked by 5 ms long current injections (1.0–1.8 nA) in each neuron every 10 s throughout the entire experiment, except during induction (see below). During baseline, APs were displaced by at least 700 ms relative to each other, to avoid accidental induction of long-term plasticity. Experiments were terminated or later discarded if membrane potential changed more than 8 mV or input resistance (measured from 250 ms long 25 pA hyperpolarizing pulses in each sweep) changed more than 30%.

Unless otherwise specified, the plasticity induction protocol consisted of pairing 5 APs at 50 Hz in the pre- and the postsynaptic cells, with pre- leading post- by +10 ms, repeated 15 times every 10 s. The 50 Hz induction frequency was chosen because it yields a maximal amount of timing-dependent LTP in L5-to-L5 pairs (Markram et al., 1997b; Sjöström et al., 2001), so it was likely to highlight proximal-distal differences in plasticity; we note that other induction protocols may result in more or less of a proximal-distal difference. In particular, induction above the critical frequency for distal $Ca^{2+}$ spikes (Larkum et al., 1999a) is likely not to adhere to the learning rule we propose here. After the induction, baseline was resumed for as long as possible. In extracellular stimulation experiments, we employed the same procedure, substituting one extracellular stimulation event for every presynaptic AP evoked in the corresponding paired recording.

### Analysis and Statistics

Plasticity experiments shorter than 40 min were not included. Amounts of potentiation and depression were measured as previously described (Sjöström et al., 2001, 2003, 2004): the average response starting 10 min after the induction until the end of the recording was divided by the average response obtained during the initial baseline period. EPSP rise time was measured as the time between 20% and 80% of the peak of the pre-pairing average response.

Comparisons were made using unpaired Student's t test for equal means. Statistically significant change for a particular condition was tested by comparing it with the specified control condition. Statistically significant change in individual experiments was assessed by comparing the post-pairing period to the baseline period. Means are reported as ± SEM. All curve fits were done by least-square gradient descent in Igor Pro. A sigmoidal fit and a sliding t test were used as independent methods to find the threshold for LTP (Figure 4C; also see text). The sliding t test was performed as previously described (Sjöström et al., 2001): The sliding threshold $d_t$ was varied between 0.25 and 3 mV, and a t test was performed for data points above and below $d_t$. A distinct minimum p value for which $p < 0.001$ suggested a threshold at the corresponding $d_t$ value.

### Two-Photon Laser-Scanning Microscopy

All imaging experiments were performed using a custom-built two-photon microscope (Prairie Technologies, Middleton, WI) with a Ti:Sapphire laser (MaiTai, Spectra-Physics) tuned to 800–840 nm. Data was acquired using ScanImage software (Pologruto et al., 2003) running in Matlab (MathWorks, Natick, MA). $Ca^{2+}$ imaging was begun about 1 hr after break-in, to allow for dye wash-in and diffusional equilibration. $Ca^{2+}$ responses were measured by line scans (2.3 ms/line, 256 or 512 lines) of the change in green fluorescence of the $Ca^{2+}$-sensitive dye Fluo-5F normalized to red $Ca^{2+}$-insensitive Alexa 594 fluorescence (dG/R). We note that the choice of Fluo-5F is appropriate for examining bAP-induced $Ca^{2+}$ influx in L5 neurons (Yasuda et al., 2004), but is less ideal for relatively small $Ca^{2+}$ influx due to subthreshold activity, so the absence of $Ca^{2+}$ signal due to EPSPs alone does not suggest that there is no $Ca^{2+}$ influx (Figure 7D, cf. Markram and Sakmann, 1994). To account for possible bleaching, we interleaved line scan conditions (e.g., in Figure 7C: first "APs," then "Depol," then "Both") and repeated them a minimum of six times each every 7–10 s. $Ca^{2+}$ traces in Figures 7C and 7D are filtered versions of line scan averages (7 point box filter). The order of line scan positions (Figures 7C–7E) was approximately randomized. The threshold for AP-EPSP-induced supralinear $Ca^{2+}$ signals (see text) was determined just below the first apical dendritic branch point. $Ca^{2+}$ signals were extracted from individual, unfiltered line scan traces, and measured in a 10–25 ms window centered on the peak of the filtered line scan average. Cell morphologies (e.g., Figures 1A and 1B) are pseudocolored maximum intensity projections (3D rendered using OsiriX; Rosset et al., 2004) of anisotropic diffusion-filtered (Broser et al., 2004) red Alexa fluorescence stacks. Dendritic diameters (Figure S2) were measured by Gaussian fits to Alexa fluorescence linescans perpendicular to the dendrite and taking the half-width as the dendritic diameter. This approach was validated in a neuron reconstructed using Neurolucida (see below). Diameters ranged between 0.8–5.0 μm, above the resolution limit of 2PLSM.

### Neuronal Reconstructions and Computer Modeling

Putative synaptic contacts were identified by axonal-dendritic crossover points (<1 μm separation), either using 2PLSM imaging of Alexa-filled cells in acute slices (see Figure S1) or using bright-field microscopy with a 100x oil objective (N.A. 1.3, Olympus BX51, Olympus, Melville, NY) of neurons histologically processed for biocytin (see above and Figure 2), or both. Neurons were reconstructed using Neurolucida (MicroBrightField Inc., Magdeburg, Germany) with a 40x objective.

Compartmental modeling was performed using the NEURON simulation environment (Hines and Carnevale, 1997) using a detailed 3D reconstruction of an L5 pyramidal neuron. Passive parameters were $C_m = 1\ \mu F/cm^2$, $R_m = 50\ k\Omega cm^2$, with $V_{rest} = -70$ mV. Spines were accounted for by scaling dendritic membrane capacitance and conductances by a factor of two (Holmes, 1989; Shelton, 1985). Synapses were placed at a range of dendritic locations and consisted of identical AMPA conductances with $E_{rev} = 0$ mV, $g_{max} = 1$ nS, $\tau_{rise} = 0.2$ ms, and $\tau_{decay} = 1.7$ ms (Häusser and Roth, 1997). $R_i$ (182 Ωcm) was adjusted by fitting the model 20%–80% EPSP rise time to the EPSP rise time from the actual paired recording (Figures 2A and 2C), assuming equal contribution from each putative synaptic contact. For the range of anatomically identified synaptic contacts at L2/3-to-L5 connections (Figure 2E), the simulated somatic EPSP amplitudes ranged from 0.16–0.59 mV, which is comparable to the L2/3-to-L5 unitary EPSP amplitudes of actual recordings (0.42 ± 0.10 mV, n = 21). We also made compartmental models from two additional L5 pyramidal cell morphologies using the same approach, and we obtained similar results. Time step for all simulations was 10 μs.

### Supplemental Data

The Supplemental Data for this article can be found online at http://www.neuron.org/cgi/content/full/51/2/227/DC1/.

### Acknowledgments

We thank Alanna Watt, Arnd Roth, Kazuo Kitamura, Mickey London, Niraj Desai, and Julian Jack for help and useful discussions, and Latha Ramakrishnan for assistance with histology and Neurolucida reconstructions. This work was supported by grants from the Wellcome Trust and the Gatsby Foundation. P.J.S. was supported by a Marie Curie Intra-European Fellowship.

Received: January 12, 2006
Revised: May 2, 2006
Accepted: June 19, 2006
Published: July 19, 2006

### References

Artola, A., Bröcher, S., and Singer, W. (1990). Different voltage-dependent thresholds for inducing long-term depression and long-term potentiation in slices of rat visual cortex. Nature *347*, 69–72.

Bekkers, J.M. (2000). Properties of voltage-gated potassium currents in nucleated patches from large layer 5 cortical pyramidal neurons of the rat. J. Physiol. *525*, 593–609.

Bernard, C., and Johnston, D. (2003). Distance-dependent modifiable threshold for action potential back-propagation in hippocampal dendrites. J. Neurophysiol. *90*, 1807–1816.

Broser, P.J., Schulte, R., Lang, S., Roth, A., Helmchen, F., Waters, J., Sakmann, B., and Wittum, G. (2004). Nonlinear anisotropic diffusion filtering of three-dimensional image data from two-photon microscopy. J. Biomed. Opt. *9*, 1253–1264.

Coogan, T.A., and Burkhalter, A. (1990). Conserved patterns of cortico-cortical connections define areal hierarchy in rat visual cortex. Exp. Brain Res. *80*, 49–53.

Cummings, J.A., Mulkey, R.M., Nicoll, R.A., and Malenka, R.C. (1996). $Ca^{2+}$ signaling requirements for long-term depression in the hippocampus. Neuron *16*, 825–833.

Debanne, D., Gähwiler, B.H., and Thompson, S.M. (1996). Cooperative interactions in the induction of long-term potentiation and depression of synaptic excitation between hippocampal CA3–CA1 cell pairs in vitro. Proc. Natl. Acad. Sci. USA *93*, 11225–11230.

Destexhe, A., Rudolph, M., and Pare, D. (2003). The high-conductance state of neocortical neurons in vivo. Nat. Rev. Neurosci. *4*, 739–751.

Froemke, R.C., Poo, M.M., and Dan, Y. (2005). Spike-timing-dependent synaptic plasticity depends on dendritic location. Nature *434*, 221–225.

Gatley, S.J., Gifford, A.N., Volkow, N.D., Lan, R., and Makriyannis, A. (1996). $^{123}$I-labeled AM251: a radioiodinated ligand which binds in vivo to mouse brain cannabinoid $CB_1$ receptors. Eur. J. Pharmacol. *307*, 331–338.

Goldberg, J., Holthoff, K., and Yuste, R. (2002). A problem with Hebb and local spikes. Trends Neurosci. *25*, 433–435.

Golding, N.L., and Spruston, N. (1998). Dendritic sodium spikes are variable triggers of axonal action potentials in hippocampal CA1 pyramidal neurons. Neuron *21*, 1189–1200.

Golding, N.L., Staff, N.P., and Spruston, N. (2002). Dendritic spikes as a mechanism for cooperative long-term potentiation. Nature *418*, 326–331.

Hansel, C., Artola, A., and Singer, W. (1997). Relation between dendritic $Ca^{2+}$ levels and the polarity of synaptic long-term modifications in rat visual cortex neurons. Eur. J. Neurosci. *9*, 2309–2322.

Häusser, M., and Roth, A. (1997). Estimating the time course of the excitatory synaptic conductance in neocortical pyramidal cells using a novel voltage jump method. J. Neurosci. *17*, 7606–7625.

Hebb, D.O. (1949). The Organization of Behavior (New York: Wiley).

Hines, M.L., and Carnevale, N.T. (1997). The NEURON simulation environment. Neural Comput. *9*, 1179–1209.

Hoffman, D.A., and Johnston, D. (1999). Neuromodulation of dendritic action potentials. J. Neurophysiol. *81*, 408–411.

Hoffman, D.A., Magee, J.C., Colbert, C.M., and Johnston, D. (1997). $K^+$ channel regulation of signal propagation in dendrites of hippocampal pyramidal neurons. Nature *387*, 869–875.

Holmes, W.R. (1989). The role of dendritic diameters in maximizing the effectiveness of synaptic inputs. Brain Res. *478*, 127–137.

Katz, L.C., and Shatz, C.J. (1996). Synaptic activity and the construction of cortical circuits. Science *274*, 1133–1138.

Koester, H.J., and Sakmann, B. (1998). Calcium dynamics in single spines during coincident pre- and postsynaptic activity depend on relative timing of back-propagating action potentials and subthreshold excitatory postsynaptic potentials. Proc. Natl. Acad. Sci. USA *95*, 9596–9601.

Korngreen, A., and Sakmann, B. (2000). Voltage-gated K+ channels in layer 5 neocortical pyramidal neurones from young rats: subtypes and gradients. J. Physiol. *525*, 621–639.

Larkum, M.E., Kaiser, K.M.M., and Sakmann, B. (1999a). Calcium electrogenesis in distal apical dendrites of layer 5 pyramidal cells at a critical frequency of back-propagating action potentials. Proc. Natl. Acad. Sci. USA *96*, 14600–14604.

Larkum, M.E., Zhu, J.J., and Sakmann, B. (1999b). A new cellular mechanism for coupling inputs arriving at different cortical layers. Nature *398*, 338–341.

Larkum, M.E., Zhu, J.J., and Sakmann, B. (2001). Dendritic mechanisms underlying the coupling of the dendritic with the axonal action potential initiation zone of adult rat layer 5 pyramidal neurons. J. Physiol. *533*, 447–466.

Levy, W.B., and Steward, O. (1979). Synapses as associative memory elements in the hippocampal formation. Brain Res. *175*, 233–245.

Linden, D.J. (1999). The return of the spike: postsynaptic action potentials and the induction of LTP and LTD. Neuron *22*, 661–666.

Lisman, J., and Spruston, N. (2005). Postsynaptic depolarization requirements for LTP and LTD: a critique of spike timing-dependent plasticity. Nat. Neurosci. *8*, 839–841.

Magee, J.C., and Johnston, D. (1997). A synaptically controlled, associative signal for Hebbian plasticity in hippocampal neurons. Science *275*, 209–213.

Malenka, R.C., and Nicoll, R.A. (1999). Long-term potentiation–a decade of progress? Science *285*, 1870–1874.

Markram, H., and Sakmann, B. (1994). Calcium transients in dendrites of neocortical neurons evoked by single subthreshold excitatory postsynaptic potentials via low-voltage-activated calcium channels. Proc. Natl. Acad. Sci. USA *91*, 5207–5211.

Markram, H., Lübke, J., Frotscher, M., Roth, A., and Sakmann, B. (1997a). Physiology and anatomy of synaptic connections between thick tufted pyramidal neurones in the developing rat neocortex. J. Physiol. *500*, 409–440.

Markram, H., Lübke, J., Frotscher, M., and Sakmann, B. (1997b). Regulation of synaptic efficacy by coincidence of postsynaptic APs and EPSPs. Science *275*, 213–215.

McNaughton, B.L., Douglas, R.M., and Goddard, G.V. (1978). Synaptic enhancement in fascia dentata: cooperativity among coactive afferents. Brain Res. *157*, 277–293.

Pologruto, T.A., Sabatini, B.L., and Svoboda, K. (2003). ScanImage: flexible software for operating laser scanning microscopes. Biomed. Eng. Online: http://www.biomedical-engineering-online.com/content/2/1/13.

Rall, W. (1967). Distinguishing theoretical synaptic potentials computed for different soma-dendritic distributions of synaptic input. J. Neurophysiol. *30*, 1138–1168.

Redman, S., and Walmsley, B. (1983). The time course of synaptic potentials evoked in cat spinal motoneurones at identified group Ia synapses. J. Physiol. *343*, 117–133.

Rosset, A., Spadola, L., and Ratib, O. (2004). OsiriX: an open-source software for navigating in multidimensional DICOM images. J. Digit. Imaging *17*, 205–216.

Rumsey, C.C., and Abbott, L.F. (2004). Equalization of synaptic efficacy by activity- and timing-dependent synaptic plasticity. J. Neurophysiol. *91*, 2273–2280.

Schiller, J., Schiller, Y., Stuart, G., and Sakmann, B. (1997). Calcium action potentials restricted to distal apical dendrites of rat neocortical pyramidal neurons. J. Physiol. *505*, 605–616.

Shelton, D.P. (1985). Membrane resistivity estimated for the Purkinje neuron by means of a passive computer model. Neuroscience *14*, 111–131.

Sjöström, P.J., and Nelson, S.B. (2002). Spike timing, calcium signals and synaptic plasticity. Curr. Opin. Neurobiol. *12*, 305–314.

Sjöström, P.J., Turrigiano, G.G., and Nelson, S.B. (2001). Rate, timing, and cooperativity jointly determine cortical synaptic plasticity. Neuron *32*, 1149–1164.

Sjöström, P.J., Turrigiano, G.G., and Nelson, S.B. (2003). Neocortical LTD via coincident activation of presynaptic NMDA and cannabinoid receptors. Neuron *39*, 641–654.

Sjöström, P.J., Turrigiano, G.G., and Nelson, S.B. (2004). Endocannabinoid-dependent neocortical layer-5 LTD in the absence of postsynaptic spiking. J. Neurophysiol. *92*, 3338–3343.

Song, S., Sjöström, P.J., Reigl, M., Nelson, S., and Chklovskii, D.B. (2005). Highly nonrandom features of synaptic connectivity in local cortical circuits. PLoS Biol. *3*, e68. 10.1371/journal.pbio.0030068.

Sourdet, V., and Debanne, D. (1999). The role of dendritic filtering in associative long-term synaptic plasticity. Learn. Mem. *6*, 422–447.

Stuart, G., Spruston, N., Sakmann, B., and Häusser, M. (1997). Action potential initiation and backpropagation in neurons of the mammalian CNS. Trends Neurosci. *20*, 125–131.

Stuart, G.J., and Sakmann, B. (1994). Active propagation of somatic action potentials into neocortical pyramidal cell dendrites. Nature *367*, 69–72.

Stuart, G.J., and Häusser, M. (2001). Dendritic coincidence detection of EPSPs and action potentials. Nat. Neurosci. *4*, 63–71.

Thomson, A.M., and Bannister, A.P. (1998). Postsynaptic pyramidal target selection by descending layer III pyramidal axons: dual intracellular recordings and biocytin filling in slices of rat neocortex. Neuroscience *84*, 669–683.

Watanabe, S., Hoffman, D.A., Migliore, M., and Johnston, D. (2002). Dendritic $K^+$ channels contribute to spike-timing dependent long-term potentiation in hippocampal pyramidal neurons. Proc. Natl. Acad. Sci. USA *99*, 8366–8371.

Waters, J., and Helmchen, F. (2004). Boosting of action potential backpropagation by neocortical network activity in vivo. J. Neurosci. *24*, 11127–11136.

Williams, S.R., and Stuart, G.J. (2000). Backpropagation of physiological spike trains in neocortical pyramidal neurons: implications for temporal coding in dendrites. J. Neurosci. *20*, 8238–8246.

Williams, S.R., and Stuart, G.J. (2002). Dependence of EPSP efficacy on synapse location in neocortical pyramidal neurons. Science *295*, 1907–1910.

Williams, S.R., and Stuart, G.J. (2003). Role of dendritic synapse location in the control of action potential output. Trends Neurosci. *26*, 147–154.

Yasuda, R., Nimchinsky, E.A., Scheuss, V., Pologruto, T.A., Oertner, T.G., Sabatini, B.L., and Svoboda, K. (2004). Imaging calcium concentration dynamics in small neuronal compartments. Sci. STKE, http://stke.sciencemag.org/cgi/content/full/OC_sigtrans;stke.2192004pl5.

Yuste, R., and Denk, W. (1995). Dendritic spines as basic functional units of neuronal integration. Nature *375*, 682–684.